Binding energy of the donor impurities in GaAs–$Ga_{1-x}Al_xAs$ quantum well wires with Morse potential in the presence of electric and magnetic fields*

Esra Aciksoz[1], Orhan Bayrak[1,†], and Asim Soylu[2]

[1] *Department of Physics, Akdeniz University, 07058, Antalya, Turkey*
[2] *Department of Physics, Nigde University, 51240, Nigde, Turkey*

(Received 1 February 2016; revised manuscript received 4 May 2016; published online 25 August 2016)

The behavior of a donor in the GaAs–$Ga_{1-x}Al_xAs$ quantum well wire represented by the Morse potential is examined within the framework of the effective-mass approximation. The donor binding energies are numerically calculated for with and without the electric and magnetic fields in order to show their influence on the binding energies. Moreover, how the donor binding energies change for the constant potential parameters (D_e, r_e, and a) as well as with the different values of the electric and magnetic field strengths is determined. It is found that the donor binding energy is highly dependent on the external electric and magnetic fields as well as parameters of the Morse potential.

Keywords: Morse potential, electric field, magnetic field, the donor atom, quantum well wire

PACS: 03.65.Ge, 03.50.De, 41.20.–q **DOI:** 10.1088/1674-1056/25/10/100302

1. Introduction

During the last decade, especially, with the development of low-dimensional semiconductor structures such as quantum wells (QWs), quantum well wires (QWWs), and quantum dots (QDs), numerous studies have been performed to investigate the hydrogenic impurity states in semiconductor structures. Understanding the effects of the impurities on the electronic properties of the semiconductors is very important for their applications in electronics and optoelectronics devices. In particular, the external electric or magnetic fields play a vital role on the band structure of the system causing a considerable change on the energy spectra and binding energies of the donor atoms. In this paper, we investigate the influence of the external fields and the confining potential shape on the binding energy of the hydrogenic donor in a quantum well wire which is made of GaAs surrounded by $Ga_{1-x}Al_xAs$ for several quantum numbers. This configuration is often used for the investigation of the electron transportation in QWW.[1]

With the development of experimental techniques and analytical methods, a great number of papers related to the hydrogenic impurity states in QWs, QWWs, and QDs have been published.[2–39] A significant number of these works were devoted to the study of the binding energy of hydrogen impurities in GaAs–$Ga_{1-x}Al_xAs$ QWW structures both experimentally and theoretically.[40–43] The impurity-limited mobility in semi-conducting wires was first investigated by Sakaki.[44] Shortly after, Petroff *et al.*[45] fabricated GaAs–AlAs quantum-well wires by molecular beam epitaxy and examined some of their optical properties experimentally. The understanding of the effect of the impurities in such systems on the electronic and optical properties is very crucial because they have a certain potential as new alternative structures for high speed devices.

The influence of several external factors, such as electric and magnetic fields, on the binding energy of impurity states in semiconductor structures have been studied by many researchers. The investigation of the effects of external factors on the binding energy of the confined system is one of the interesting subjects from both the theoretical and technological points of view. In this respect, many studies have been performed on the electric,[2–5] the magnetic fields,[6–10] and their combined effects,[11] the hydrostatic pressure[12,13] and the temperature dependence[14,15] of the binding energy in these systems. In certain theoretical studies related to different low-dimensional semiconductor structures, different confinement potentials denote that the donor binding energy decreases as a function of external electric field.[16–19] Most recently, Ghazi *et al.* have investigated the effects of the external electric fields on the (In,Ga)NGaN spherical quantum dots by using the Ritz variational method based on the effective-mass approximation and finite potential.[20] Erdogan *et al.* have studied the effects of both the external electric and magnetic fields on the self-polarization and binding energy of hydrogenic impurity confined in an infinite quantum wire.[21] Rezaei *et al.*[22] have investigated the combined effects of hydrostatic pressure and an external electric field on the binding energy and the self-polarization of a hydrogenic impurity in a finite confining potential square QWW. In Refs. [23]–[27], the combined ef-

*Project supported by the Turkish Science Research Council (TÜBİTAK) and the Financial Supports from Akdeniz and Nigde Universities.
†Corresponding author. E-mail: bayrak@akdeniz.edu.tr
© 2016 Chinese Physical Society and IOP Publishing Ltd

fects of these factors on the binding energy of impurity states have also been studied. Rezaei *et al.*[28] have also investigated the simultaneous effects of the external electric field, hydrostatic pressure and temperature on the off-center donor impurity binding energy in a spherical Gaussian QD by using the effective-mass approximation within a matrix diagonalization scheme. More recently, Baghramyan *et al.*[29] have investigated the effects of hydrostatic pressure, temperature, aluminum concentration and impurity position on hydrogen-like donor binding energy in GaAs/$Ga_{1-x}Al_xAs$ concentric double quantum rings. All studies mentioned above have shown that external factors play a crucial role for the investigations of the binding energy of a donor.

In low-dimensional heterostructure, the binding energy and other characteristic properties of the impurity depend on the shape of the confining potential. For this reason, the authors have studied many different types of confining potential in their studies. In Refs. [30]–[32], they have used the effective-mass approximation and a variational procedure in order to calculate the binding energy of a donor impurity inside a square finite depth quantum well. They have studied the effects of hydrostatic pressure on the electronic states and the binding energies of donor impurity. Simultaneous effects of hydrostatic pressure and the temperature on the donor impurity in a Pöschl–Teller quantum well have been investigated in Refs. [33] and [34]. Hakimyfard *et al.*[35] have studied the effects of hydrostatic pressure and magnetic field on intersubband optical transitions in a Pöschl–Teller quantum well. Recently, Barseghyan *et al.*[36] have considered the effects of electric and magnetic fields as well as hydrostatic pressure on the donor binding energy in Pöschl–Teller quantum rings. Bose[37] has used perturbation method to calculate the binding energies of the donor impurity states in spherical QDs with parabolic confinement. Murillo and Montenegro[38] have calculated the binding energy of a donor impurity in GaAs–$Ga_{1-x}Al_xAs$ spherical QD with parabolic confinement for the existence of an applied electric field. Very recently, Akankan studied the effect of a spatial electric field on the binding energy and polarization of a donor impurity in a GaAs/AlAs tetragonal quantum dot.[39] In this study, the authors have performed an infinite confining potential calculation within the effective-mass approximation by using the variational procedure. For this physical system, the authors have studied the effects of different confining potential shapes on the binding energy of the donor.[39]

On the other hand, another potential model is the Morse potential which has been considered over the years and it has been used as one of the most useful models to describe the interaction between two atoms in diatomic molecules. The Schrödinger equation with the Morse potential has been solved by using the super-symmetry (SUSY),[46] the Nikiforov–Uvarov method (NU),[47] the hypervirial perturbation method (HV),[48] the shifted and modified shifted $1/N$ expansion methods[49] as well as the variational method.[50] To the best of our knowledge, there has been no previous study in which the use of Morse potential has been considered as a confining potential in order to explain the behavior of the binding energy of a donor in a semiconductor. In this respect, the aim of this study is to understand the influence of the parameters of the Morse type confining potential and electric or magnetic fields on the binding energy of the donor in a quantum well wire (QWW) within the framework of the effective-mass approximation by using the Runge–Kutta method.

In the next section, we present the theoretical framework of the model and the numerical solution method called Runge–Kutta. Our numerical results are presented and discussed in Section 3. Finally, we give our conclusion and summary in Section 4.

2. Theoretical analysis

The Hamiltonian for a charged particle moving in the constant magnetic and linear electric fields can be written as

$$H = \frac{1}{2m^*}(\boldsymbol{p} - \frac{q}{c}\boldsymbol{A})^2 + U(r), \tag{1}$$

where m^* is the mass, q is the electric charge, $\boldsymbol{p}$ is the momentum of the particle, $\boldsymbol{A}$ is the vector potential, and $U(r) = \varepsilon r$ is the linear electric field potential. Here, ε is the strength of the electric field. If the vector potential in the symmetric gauge is chosen as $\boldsymbol{A} = -(1/2)(\boldsymbol{r} \times \boldsymbol{B})$ with a uniform magnetic field $\boldsymbol{B} = B\hat{k}$

$$H = -\frac{\hbar^2}{2m^*}\nabla^2 - \frac{qB}{2m^*}L_z + \frac{q^2B^2}{8m^*}(x^2+y^2) + U(r) + V(r), \tag{2}$$

$\omega_c = qB/m^*$ is the cyclotron frequency and $V(r)$ is the confinement potential induced by QWW

$$H = -\frac{\hbar^2}{2m^*}\nabla^2 - \frac{1}{2}\omega_c L_z + \frac{1}{8}m^*\omega_c^2 r^2 + \varepsilon r + V(r), \tag{3}$$

and the Schrödinger equation becomes

$$\begin{aligned}\widehat{H}\psi(\boldsymbol{r}) &= \left[-\frac{\hbar^2}{2m^*}\nabla^2 - \frac{1}{2}\omega_c L_z + \frac{1}{8}m^*\omega_c^2 r^2 + \varepsilon r + V(r)\right]\psi(\boldsymbol{r}) \\ &= E\psi(\boldsymbol{r}),\end{aligned} \tag{4}$$

where ∇^2 is the two-dimensional Laplacian and L_z is the angular momentum operator, $-\mathrm{i}\hbar\mathrm{d}/\mathrm{d}\phi$, with eigenvalue $\hbar m$. In the polar coordinates (r, ϕ) using the following eigenfunction

$$\Psi(\boldsymbol{r}) = \frac{e^{\mathrm{i}m\phi}}{\sqrt{2\pi}}\frac{R(r)}{\sqrt{r}}. \tag{5}$$

According to the effective mass theory (EMT), the radial Schrödinger equation for the donor in a spherical quantum dot (SQD) is given by

$$\frac{\mathrm{d}^2R}{\mathrm{d}r^2}+\frac{2m^*}{\hbar^2}\left[E-\frac{1}{2}\omega_c\hbar m-\frac{(m^2-1/4)\hbar^2}{2m^*r^2}-\frac{1}{8}m^*\omega_c^2r^2+\frac{eZ_d}{\varepsilon r}-V(r)-\varepsilon r\right]R(r)=0, \tag{6}$$

where Z_d is the donor charge number. In this paper, the reduced atomic units are used so that energies are calculated in units of effective Rydberg R_{y^*} and correspond to a length unit of one effective Bohr radius a_{0^*}. The R_{y^*} and a_{0^*} can be determined by $R_{y^*}=m^*e^4/2\hbar^2\varepsilon^2=5.72$ meV and $a_{0^*}=\hbar^2\varepsilon/m^*e^2\cong 100$ Å, where m^* and ε are, respectively, the electron effective mass, $m^*\cong 0.065m_e$ and dielectric constant of GaAs material, $\varepsilon=12.4$, respectively. In SI units 1 a.u. of the reduced electric and magnetic field strengths is $\varepsilon^*=R_{y^*}/ea_{0^*}=5.71\times10^5$ V·m^{-1}·a.u.$^{-1}$ as well as $B^*=\hbar/e(a_{0^*})^2=6.567$ T·a.u.$^{-1}$. As it is seen from Eq. (6), in order to be able to investigate two-dimensional donor binding energy in an electromagnetic field, we need to solve the radial Schrödinger equation for the following type of effective potential

$$V_{\mathrm{eff}}(r)=\frac{(m^2-1/4)\hbar^2}{2m^*r^2}+\frac{1}{8}m^*\omega_c^2r^2-\frac{eZ_d}{\varepsilon r}+\varepsilon r+V(r), \tag{7}$$

where $V(r)$ is the donor confining potential and it is chosen as follows:[46–51]

$$V_{\mathrm{Morse}}(r)=D_e(\mathrm{e}^{-2\alpha x}-2\mathrm{e}^{-\alpha x}), \tag{8}$$

with $x=(r-r_e)/r_e$ and $\alpha=ar_e$. Here, D_e and α denote the dissociation energy and Morse parameter, respectively. r_e is the equilibrium distance (bound length) between nuclei and a is a parameter to control the width of potential well. The term $[(m^2-1/4)\hbar^2]/2m^*r^2$ comes from the two-dimensional motion and behaves like a centrifugal potential. The radial Schrödinger equation for the effective potential in Eq. (7) is given by

$$\frac{\mathrm{d}^2R}{\mathrm{d}r^2}+\frac{2m^*}{\hbar^2}[E_n-V_{\mathrm{eff}}(r)]R(r)=0, \tag{9}$$

where

$$E_n=E-(1/2)\omega_c\hbar m.$$

The donor binding energy for any quantum state may be taken as the difference in energy between eigenvalues in the absence of the donor atom ($Z_d=0$) and that in its presence ($Z_d=1$)

$$E_b(\ell)=E_{n\ell}(Z_d=0)-E_{n\ell}(Z_d=1). \tag{10}$$

The model potential, which consists of $1/r^2+r^2-1/r+r+(\mathrm{e}^{-2r}-\mathrm{e}^{-r})$ terms, cannot be solved analytically. Thus, we have to use either approximation such as perturbation, variation, etc., or numerical methods (Runge–Kutta, Numerov, etc.). In this study, we have solved the Schrödinger equation for Eq. (7) by using the Runge–Kutta 4-th order method.

The following ordinary first order differential equation can be solved by using the Runge–Kutta method[52]

$$\frac{\mathrm{d}y}{\mathrm{d}x}=f(x,y),\quad y(0)=y_0. \tag{11}$$

According to the Runge–Kutta method, the solution of Eq. (11) is

$$y_{n+1}=y_n+\frac{1}{6}h(k_1+2k_2+2k_3+k_4), \tag{12}$$

$$x_{n+1}=x_n+h,\ \ n=0,1,2,\ldots \tag{13}$$

in terms of

$$\begin{aligned}k_1&=f(x_n,y_n),\\ k_2&=f\left(x_n+\frac{1}{2}h,y_n+\frac{1}{2}hk_1\right),\\ k_3&=f\left(x_n+\frac{1}{2}h,y_n+\frac{1}{2}hk_2\right),\\ k_4&=f(x_n+h,y_n+hk_3),\end{aligned} \tag{14}$$

where h is the step size, and we used $h=0.05$ in the calculations. In order to apply the Runge–Kutta method to the Schrödinger equation which is the second order, we rewrite the Schrödinger equation as the first-order one so that we have the two coupled first order linear ordinary differential equations. Let us take $\mathrm{d}R(r)/\mathrm{d}r=\chi(r)$, and then we have $\mathrm{d}^2R(r)/\mathrm{d}r^2=\mathrm{d}\chi(r)/\mathrm{d}r$. Therefore the second-order Schrödinger equation is reduced to the coupled first-order linear differential equations as follows:

$$\begin{aligned}&\frac{\mathrm{d}R(r)}{\mathrm{d}r}=\chi(r),\qquad R(0)=0,\\ &\frac{\mathrm{d}\chi(r)}{\mathrm{d}r}+\frac{2m^*}{\hbar^2}[E_n-V_{\mathrm{eff}}(r)]R(r)=0,\quad \chi(0)=1.\end{aligned} \tag{15}$$

Integrating of the Schrödinger equation from $r_{\min}=0$ to $r_{\max}=25$ Å with the quantum mechanical boundary conditions of the wave function which are $R(0)=0$ and $R(r_{\max})=0$, we can calculate the correct energy eigenvalues by using the bisections method. In the calculations, we determine the radial node of the wave functions by searching $R(r)*R(r+h)<0$ for the integration range. The energy eigenvalues are determined in terms of the wave functions satisfying both boundary conditions and radial number of nodes.

3. Numerical results

In Fig. 1, the influence of m quantum number and the external applied electric and magnetic fields on the effective potential is shown. As can be seen in Fig. 1, when m is increased, the forms of the potential pocket shown as black lines in Fig. 1 remain almost the same for $m=0$, 1, and 2. For $m=1$, when

the magnetic field is applied, the width of the potential pocket becomes narrower. Moreover, as the strength of the magnetic field increases, the potential pocket turns to a harmonic oscillator for higher ω_c values. This situation can be understood with the magnetic field represented by the harmonic oscillator in Eq. (7). At the higher Larmor frequencies, since the harmonic oscillator term is more dominant than other terms in the effective potential, the system behaves as an harmonic oscillator. When the electric field is chosen as the positive direction, the width of the potential pocket becomes wider. However, when the electric field is in the negative direction, the width of the potential pocket narrows.

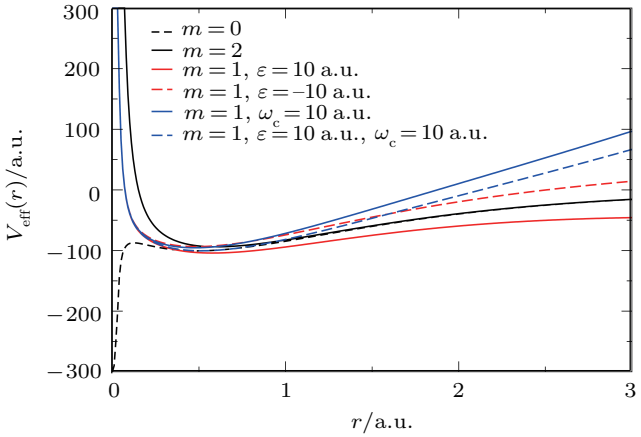


Fig. 1. (color online) The effective potential versus r for several quantum numbers, the external electric and magnetic fields.

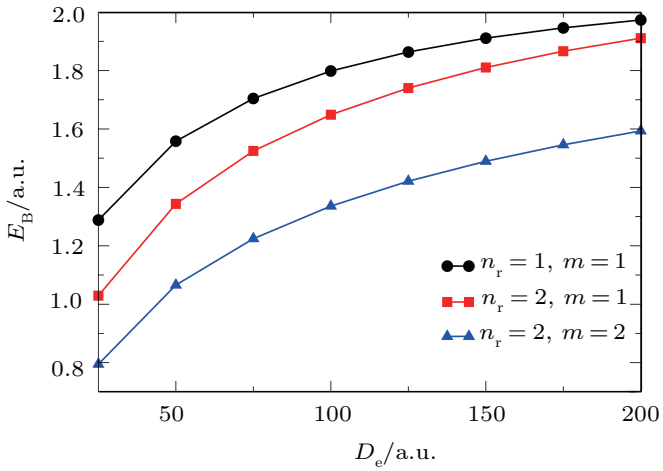


Fig. 2. (color online) The binding energies versus different D_e values.

In Figs. 2, 3, and 4, we present our results for the binding energy as a function of depth of the potential, equilibrium distance and potential width, respectively. In order to give a clear picture of both electric and magnetic field effects on the binding energy, we also present the cases for without the electric and magnetic fields for the confining potential parameters (D_e, r_e, and a) for several quantum numbers. The obtained results show that the binding energy increases as the potential depth (D_e) increases, as seen in Fig. 2. When the potential depth increases, the ground state of the donor has a larger negative energy eigenvalue and hence the binding energy increases. But, when the radial node and angular momentum quantum numbers are increased, the binding energy of the donor decreases with increasing of these numbers as expected. The binding energy decreases approximately exponentially with the increasing of the equilibrium distance (r_e) and the binding energy of the donor almost remains the same with increasing the quantum numbers and r_e values in Fig. 3.

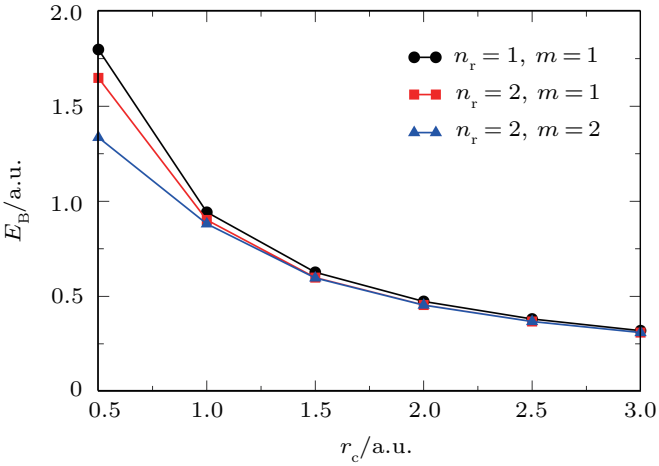


Fig. 3. (color online) The binding energies versus different r_e values.

The reason for this decreasing of the binding energy of the donor is the decreasing of the potential depth with increasing the equilibrium distance. The binding energy of the donor increases until a certain a value (approximately $a = 1.5$) and then the binding energy decreases with increasing of the potential width (a). When we increase the radial node and angular momentum quantum numbers, the binding energy of the donor decreases with increasing these numbers in Fig. 4. The reason for this increasing and decreasing of the binding energy of the donor is the potential which strongly depends on the parameter a. Firstly when parameter a increases the depth and width of the potential increase and then the depth and width of the potential decrease. Similar behavior can be seen in the variation of the binding energy of donor versus a parameter in Fig. 4.

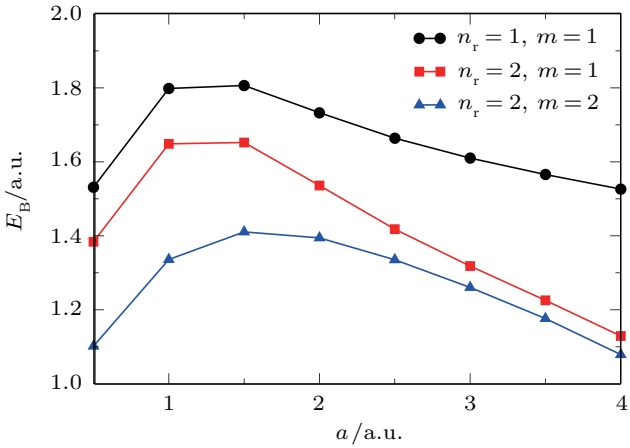


Fig. 4. (color online) The binding energies versus different a values.

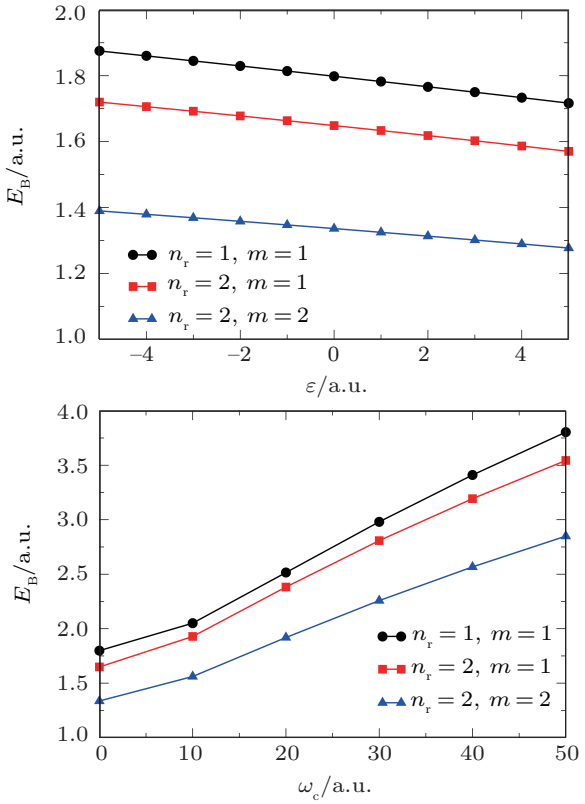


Fig. 5. (color online) The binding energies versus different electric and magnetic field (a.u).

In Fig. 5, we show the applied electric and magnetic field dependence of the donor binding energy for the constant values of the confining potential parameters. These parameters are $D_e = 100$ a.u., $r_e = 0.5$ a.u., and $a = 1$ a.u. In Fig. 5, the effect of the electric field on the binding energy of the donor for with and without electric field strength is shown. As can be seen from the curve in Fig. 5, it is clear that the binding energy is an increasing function of the negative electric field strength. But the binding energy is a decreasing function of the positive electric field strength. This is an expected result since if the electric field in Eq. (7) is positive, the depth of the effective potential decreases and the binding energy of the donor decreases. In contrast, if the electric field is negative, the depth of the effective potential increases and the binding energy of the donor increases as well. We have shown that the binding energy increases with increasing of the magnetic field in Fig. 5. At the higher Larmor frequencies in Eq. (7), the harmonic oscillator term becomes more dominant than the other terms. Therefore when Larmor frequencies increase, the binding energy of the donor increases.

In Table 1, we list our results for several n_r and m quantum numbers. It is clear that the binding energy decreases with increasing quantum numbers when the electric and magnetic fields are zero as well as for only the electric field being negative or positive. However, when only the magnetic field is applied does the binding energy increase with the increasing of quantum numbers, and the binding energy takes only the positive values.

Table 1. $E_{n_r m}$ values for different quantum numbers, the electric and magnetic field strengths. In the calculations, $D_e = 100$ a.u., $a = 1$ a.u., $r_e = 0.5$ a.u. are used and all other units are in unit a.u.

(n_r, m)	$\varepsilon = 0, \omega_c = 0$	$\varepsilon = -5, \omega_c = 0$	$\varepsilon = 5, \omega_c = 0$	$\varepsilon = 0, \omega_c = 20$	$\varepsilon = 0, \omega_c = 50$
(1,1)	−78.9914	−75.3713	−82.7499	−46.2349	27.4083
(2,1)	−65.8542	−61.4123	−70.4717	−22.4994	77.5060
(2,2)	−60.5107	−55.5925	−65.6244	−1.4545	127.3770
(3,1)	−53.8405	−48.5248	−59.3936	1.3268	128.3680
(3,2)	−48.8310	−43.0250	−54.9089	22.6030	178.6610
(3,3)	−43.8178	−37.5366	−50.4111	43.9174	228.8660

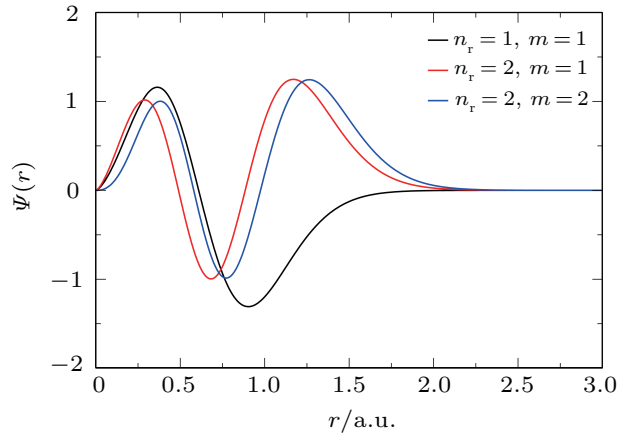


Fig. 6. (color online) Normalized wave functions for several quantum numbers.

Figure 6 shows the normalized wave function for several quantum numbers and the absence of any external electric and magnetic fields, the constant potential parameters used in our calculations are taken as the following: $D_e = 100$ a.u., $r_e = 0.5$ a.u., and $a = 1$ a.u.

4. Summary and conclusion

In this paper, we have used the Runge–Kutta method and the effective-mass approximation in order to investigate the effects of confining potential and applied electric and magnetic fields on the binding energy of donor impurity in the GaAs–$Ga_{1-x}Al_xAs$ quantum well wire. The binding energy of the donor for without the applied electric and magnetic fields is calculated. Our results can be summarized as follows. In the case of without the external fields, (i) the binding energy in-

creases with increasing the potential depth (D_e), (ii) the binding energy decreases with increasing of the equilibrium distance (r_e) and the potential width (a). In the case of the constant values of the confining potential parameters with external fields, (iii) the binding energy of the donor increases or decreases depending on the direction of the applied electric field, (iv) the binding energy increases with increasing magnetic field. Actually, the reason for the increasing of the binding energy of the donor is increasing of the depth and width of the effective potential due to the external fields. It should be noted that the parameters in Morse potential would be used for modeling some different effects which change the energies of the donor in semiconductor studies. In addition to this, the obtained results related with the external field effects on the energies might be interesting for both experimental and theoretical studies on the impurities in the field.

References

[1] Oubram O, Mora-Ramos M E and Gaggero-Sager L M 2009 *Eur. Phys. J. B* **71** 233
[2] H. Wua, H. Wanga, L. Jianga, Q. Gong, S. Feng 2009 *Physica B: Condensed Matter* **404** 122
[3] Duque C A, Mora-Ramos M E, Kasapoglu E, Sari H and Skmen I 2012 *Phys. Status Solidi B* **249** 118
[4] Safwan S A, Asmaa A S, El Meshed N, Hekmat M H, El-Sherbini T H M and Allam S H 2010 *Superlattices and Microstructures* **47** 606
[5] Jiang L, Wang H, Wu H, Gong Q and Feng S 2009 *J. Appl. Phys.* **105** 053710
[6] Panahi H, Golshahi S and Doostdar M 2013 *Physica B* **418** 47
[7] Osorioa F A P, Marques A B A, Machadoc P C M and Borges A N 2005 *Microelectronics Journal* **36** 244
[8] Sali A, Fliyou M, Satori H and Loumrhari H 2003 *J. Phys. Chem. Solids* **64** 31
[9] Akbas H, Dane C, Guleroglu A and Minez S 2009 *Physica E: Low-dimensional Systems and Nanostructures* **41** 605
[10] Balandin A and Bandyopadhyay S 1995 *Phys. Rev. B* **52** 8312
[11] Zeng Z, Garoufalis C S and Baskoutas S 2012 *J. Phys. D: Appl. Phys.* **45** 235102
[12] Peter A J 2005 *Physica E* **28** 225
[13] Rezaei G and Doostimotlagh N A 2012 *Physica E* **44** 833
[14] Kasapoglu E 2008 *Phys. Lett. A* **373** 140
[15] Khordad R 2009 *Physica E: Low-dimensional Systems and Nanostructures* **41** 543
[16] Dalgic S, Ulas M and Ozkapi B 2005 *J. Optoelectron. Adv. Mater.* **7** 2041
[17] Dalgic S and Ozkapi B 2009 *J. Optoelectron. Adv. Mater.* **11** 2120
[18] Peter A J and Navaneethakrishnan K 2008 *Superlattice Microstruct.* **43** 63
[19] Wang H, Jiang L, Gong Q and Feng S 2010 *Physica B: Condens. Matter* **405** 3818
[20] Ghazi H E, Jorio A and Zorkani I 2013 *Physica B: Conden. Matter* **426** 155
[21] Erdogan I, Akankan O and Akbas H 2006 *Physica E: Low-dimensional Systems and Nanostructures* **33** 83
[22] Rezaei G, Mousavi S and Sadeghi E 2006 *Physica B: Conden. Matter* **407** 2637
[23] Tangarife E and Duque C A 2010 *Appl. Surf. Sci.* **256** 7234
[24] Kirak M, Altinok Y and Yilmaz S 2013 *J. Lumin.* **136** 415
[25] Rezaei G and Shojaeian Kish S 2012 *Physica E: Low-dimensional Systems and Nanostructures* **45** 56
[26] Kasapoglu E, Ungan F, Sari H and Sokmen I 2010 *Physica E: Low-dimensional Systems and Nanostructures* **42** 1623
[27] Barseghyan M G, Kirakosyan A A and Duque C A 2009 *Eur. Phys. J. B* **72** 521
[28] Rezaei G, Taghizadeh S F and Enshaeian A A 2012 *Physica E: Low-dimensional Systems and Nanostructures* **44** 1562
[29] Baghramyan H M, Barseghyan M G, Duque C A and Kirakosyan A 2013 *Physica E: Low-dimensional Systems and Nanostructures* **48** 164
[30] Elabsy A M 1994 *J. Phys.: Condens. Matter* **6** 10025
[31] Raigoza N, Duque C A, Reyes-Gomez E and Oliveira L E 2006 *Phys. Status Solidi B* **243** 635
[32] Raigoza N, Morales A L, Montes A, Porras-Montenegro N and Duque C A 2004 *Phys. Rev. B* **69** 045323
[33] Hakimyfard A, Barseghyan M G, Duque C A and Kirakosyan A A 2009 *Physica B: Conden. Matter* **404** 5159
[34] Barseghyan M G, Hakimyfard A, Lopez S Y, Duque C A and Kirakosyan A A 2010 *Physica E: Low-dimensional Systems and Nanostructures* **42** 1618
[35] Hakimyfard A, Barseghyan M G and Kirakosyan A A 2009 *Physica E: Low-dimensional Systems and Nanostructures* **41** 1596
[36] Barseghyan M G, Hakimyfard A, Kirakosyan A A, Mora–Ramos M E and Duque C A 2012 *Superlattices and Microstructures* **51** 119
[37] Bose C 1999 *Physica E: Low-dimensional Systems and Nanostructures* **4** 180
[38] Murillo G and Porras-Montenegro N 2000 *Phys. Status Solidi B* **220** 187
[39] Akankan O 2013 *Superlattices and Microstructures* **55** 45
[40] Kubakaddi S S, Mulimani B G and Jali V M 1986 *J. Phys. C: Solid State Phys.* **19** 5453
[41] Tavares M R S 2005 *Phys. Rev. B* **71** 155332
[42] Hu B Y and Sarma S Das 1992 *Phys. Rev. Lett.* **68** 1750
[43] Machado P C M, Borges A N and Osório F A P 2011 *Phys. Status Solidi B* **248** 931
[44] Sakaki H 1980 *Jpn. J. Appl. Phys.* **19** L735
[45] Petroff P M, Gossard A C, Logan R A and Wiegmann W 1982 *Appl. Phys. Lett.* **41** 635
[46] Cooper F, Khare A and Sukhatme U 1995 *Phys. Rep.* **251** 267
[47] Nikiforov A F and Uvarov V B 1988 *Special Functions of Mathematical Physics* (Basel: Birkhäuser Verlag)
[48] Killingbeck J P, Grosjean A and Jolicard G 2002 *J. Chem. Phys.* **116** 447
[49] Bag M, Panja M M and Dutt R 1992 *Phys. Rev. A* **46** 9
[50] Filho E D and Ricotta R M 2000 *Phys. Lett. A* **269** 269
[51] Bayrak O and Boztosun I 2006 *J. Phys. A: Math. Gen.* **36** 6955
[52] Butcher J C 2008 *Numerical Methods for Ordinary Differential Equations* (John Wiley) p. 93